Renewable Energy 99 (2016) 1–9

Contents lists available at ScienceDirect

Renewable Energy

journal homepage: www.elsevier.com/locate/renene

Ag-coated polyurethane fibers membranes absorbed with quinary fatty acid eutectics solid-liquid phase change materials for storage and retrieval of thermal energy

Huizhen Ke [a, b], Mohy uddin Hafiz Ghulam [b], Yonggui Li [a], Jing Wang [b], Bin Peng [b], Yibing Cai [b], Qufu Wei [b, *]

[a] Fujian Engineering Research Center for Textile and Clothing, Faculty of Clothing and Design, Minjiang University, Fuzhou, Fujian, 350108, China
[b] Key Laboratory of Eco-Textiles, Ministry of Education, Jiangnan University, Wuxi, Jiangsu, 214122, China

ARTICLE INFO

Article history:
Received 30 January 2016
Received in revised form
13 April 2016
Accepted 14 June 2016

Keywords:
Magnetron sputtering
Polyurethane
Quinary fatty acid eutectic
Composite PCMs
Thermal properties
Ag nanoparticles

ABSTRACT

The novel quinary fatty acid eutectic (CA-LA-MA-PA-SA) of capric acid, lauric acid, myristic acid, palmitic acid and stearic acid was successfully prepared with the mass ratio of 61.09/24.61/8.13/4.01/2.16. Thereafter, the innovative Ag-coated polyurethane (PU) fibers membranes with different concentrations of Ag, which were selected as a supporting material to adsorb the CA-LA-MA-PA-SA eutectics, were successfully fabricated through electrospinning followed by magnetron sputter. The energy dispersive X-ray confirmed that Ag nanoclusters were successfully deposited on the surface of PU fibers as a result of sputter coating. The observations of atomic force microscope indicated that the surface roughness of the PU fibers significantly increased with increase in coating time. The scanning electron microscope images demonstrated that the CA-LA-MA-PA-SA eutectics were uniformly distributed into the three-dimensional porous structures of uncoated and Ag-coated PU fibers membranes. Furthermore, the differential scanning calorimeter curves suggested that the CA-LA-MA-PA-SA/PU/Ag composites phase change materials (PCMs) possessed melting enthalpies about 110 kJ/kg and melting temperature around 17 °C. The absorption ratios of the CA-LA-MA-PA-SA eutectic in composite PCMs was approximately at 73.74%–83.18%. The investigation on thermal performance indicated that we achieved higher melting and freezing rates of the CA-LA-MA-PA-SA/PU/Ag composites PCMs by increasing coating time. In addition to this, after depositing Ag nanoparticles the melting and freezing times of composites PCMs were shortened to about 21%–65%.

1. Introduction

Latent heat storage method using phase change materials (PCMs) is a promising technology for thermal energy storage. PCMs including solid-solid PCMs, solid-liquid PCMs, solid-gas PCMs and liquid-gas PCMs are commonly known as latent heat storage materials, which can absorb, store and release large amount of thermal energy by changing their phases during phase transition processes. Currently, PCMs have been extensively studied and successfully used in numerous applications such as solar energy systems, energy conserving in buildings, domestic solar hot water systems, environmental sensitive clothing, waste heat of condensation recovery, active and passive cooling in electronic devices, preservation of food items, heat protection system in aerospace industry, air conditioning system, low temperature refrigeration, biomedical and biological carrying systems, greenhouse applications, Li-ion batteries due to their prominent properties like lower vapor pressure and volume change, high energy storage density and small temperature change from storage to retrieval, etc [1–10].

Among the investigated PCMs, fatty acids have been considered as a potential PCMs because of their desirable and excellent characteristics like high latent heat enthalpies, narrow phase transition temperatures, non-toxicity, non-corrosive, no supercooling and phase segregation, recyclable as well as low cost [11]. However, the conventional solid-liquid PCMs (e.g., fatty acids) present some drawbacks, particularly leakage during solid-liquid phase change processes and low thermal conductivity limit their practical applications. Due to these limitations, form-stable PCMs consisting of

* Corresponding author.
E-mail address: qfwei@jiangnan.edu.cn (Q. Wei).

http://dx.doi.org/10.1016/j.renene.2016.06.033
0960-1481/

fatty acids or their eutectic mixtures and supporting materials have been rapidly developed to overcome these problems. The supporting materials are mainly polymers (e.g., PMMA [12], polystyrene [13], polypyrrole [14], styrene-methylmethacrylate (St-MMA) [15], Poly(melamine-urea-formaldehyde) [16], polyamide 6 [17], polyacrylonitrile [18], etc.) and inorganic materials (e.g., expanded graphite and carbon fibers [19], expanded perlite [20], Kaolin [21], activated-attapulgiate [22], activated montmorillonite [23], silicon dioxide [24], nitrogen-doped graphene [25], etc.), which can maintain the solid shape of materials. In addition to this, some of these inorganic materials like expanded graphite and carbon fibers [19] as well as nitrogen-doped graphene [25] can effectively improve thermal energy storage and release rates of form-stable PCMs. Furthermore, fatty acid eutectics have recently drawn wide attentions due to the fact that the phase change temperatures range of fatty acid eutectics could match with the actual climatic requirements of temperature ranges, which means that they can be applied to lower temperature thermal storage applications such as building energy storage.

However, according to the previous literature, there have been no reports about the synthesis and investigations of thermal properties of quinary fatty acid eutectics that can be selected as the low temperature solid-liquid PCMs, as well as the development of the form-stable PCMs with electrospun polyurethane (PU) fibers membranes acting as supporting material. In addition to this, magnetron sputter technology has also never been used before to improve thermal energy storage and release rates of form-stable PCMs. Magnetron sputtering is a simple, effective and environmental friendly technique with enormous advantages such as uniform and compact deposition, strong bonding between the coating and its substrate, simple operation, high productivity, low cost and suitability for industrial production as compared to other techniques that are used to enhance the thermal conductivity of PCMs [26,27]. Among the various polymers, polyurethane (PU) exhibits excellent mechanical properties, elastomeric, resistant to abrasion, good spin-ability, water insolubility and low cost, which makes it an important thermoplastic synthetic polymer material. The electrospun fibers are normally collected in the form of nanofibrous membranes and in this form they possess excellent properties such as small diameter, large surface-to-volume ratio, light weight, high porosity, three-dimensional network structure and high mechanical strength. Due to above mention properties they have great potential to be utilized as the supporting materials for the preparation of form-stable PCMs.

Therefore, in the present paper, the novel quinary fatty acid eutectic (i.e., CA-LA-MA-PA-SA) was prepared via melt blending followed by ultrasonication. After that, in order to improve the thermal storage and release rates of composite PCM, the magnetron sputter coating was applied to generate functional Ag nanostructure films with high thermal conductivity on the surface of electrospun PU fibers by using different coating times. Thereafter, the innovative series of CA-LA-MA-PA-SA/PU/Ag composite PCMs with different amount of Ag were fabricated by adsorbing the quinary fatty acid eutectic into the three-dimensional porous network structures of different Ag-coated PU fibers membranes through the effects of capillary and surface tension forces for storage and retrieval of thermal energy. For comparison, the CA-LA-MA-PA-SA/PU phase change composite fibrous membranes without the Ag sputter coating were also prepared and investigated.

2. Experimental

2.1. Materials

The capric acid (CA), lauric acid (LA), myristic acid (MA), palmitic acid (PA), stearic acid (SA) and N, *N*-dimethyl formamide (DMF) were obtained from the Sinopharm Group Chemical Reagent Co., Ltd. (Shanghai, China). The purities of purchased CA, LA, MA, PA and SA were 98.5%, 98%, 98%, 98% and 98%, respectively. The polyurethane pellets (PU, 2103-80AE) were supplied by Dow Chemical Company, USA. The chemicals were used as received without further purification.

2.2. Preparation of fatty acid eutectic mixtures

The Schrader Equation was used to calculate the theoretical eutectic mass ratios of the binary, ternary, quaternary and quinary fatty acid mixtures [28].

$$T = 1\Big/\left(1\Big/T_f - R\ln X_A\Big/\Delta_s^1 H_A\right) \quad (1)$$

Where T(K) is the melting temperature of the mixture containing compound A, X_A is the mole fraction of component A in the mixture, $\Delta_s^1 H_A$ (Jmol^{-1}) and T_f(K) are the melting enthalpy and melting temperature of compound A, and R is the gas constant (8.314 JK^{-1} mol^{-1}). The thermal characteristic data of the extrapolated peak onset temperatures (T_e), melting peak temperature (T_m), freezing peak temperature (T_c), melting enthalpy (ΔH_m) and freezing enthalpy (ΔH_c) of the five fatty acids were listed in Table 1. These data were extracted from DSC curves by using the DSC measurement analysis software. The similar method has also been reported in previous literature [29]. During the experimental process, it was found that there were marginal differences between the theoretical calculated eutectic mass ratios and the experimental determined eutectic mass ratios owing to the experimental errors of data obtaining from the DSC management and the some amounts of impurities in the individual fatty acids. The theoretically calculated eutectic mass ratios and the experimentally determined eutectic mass ratios of the prepared binary, ternary, quaternary and quinary fatty acid mixtures were summarized in Table 2.

The fatty acids with experimentally determined eutectic mass ratios were first mixed in a beaker. Then it was heated in oven at 60 °C for 2 h followed by ultrasonication in 330 W ultrasonic water bath maintained at 60 °C for 2 min. Finally, a series of binary, ternary, quaternary and quinary fatty acid eutectic mixtures were obtained after cooling them down at room temperature.

2.3. Electrospinning

The polymer solution concentration of 13 wt% were prepared by dissolving the PU pellets in *N*,*N*-Dimethylformamide (DMF) solvent. The prepared solution was spun from a 20 ml syringe with a needle of 0.3 mm diameter. The solution feed rate was set at 0.2 ml/h. The PU fibers were deposited on a grounded roller wrapped with

Table 1
The peak onset temperature (T_e), melting peak temperature (T_m), freezing peak temperature (T_c), melting enthalpy (ΔH_m) and freezing enthalpy (ΔH_c) of the five fatty acids.

Fatty acids	Melting			Freezing		
	T_e (°C)	T_m (°C)	ΔH_m (kJ/kg)	T_e (°C)	T_c (°C)	ΔH_c (kJ/kg)
CA	31.12	32.71	166.7	29.30	29.25	163.1
LA	44.02	44.63	182.3	42.09	41.73	182.4
MA	53.73	56.06	187.3	52.09	51.94	184.9
PA	62.11	64.83	212.1	60.38	59.28	214.6
SA	68.96	70.52	222.8	67.06	66.50	226.7

Table 2
The theoretically calculated eutectic mass ratios and the experimentally determined eutectic mass ratios of the prepared binary, ternary, quaternary, quinary fatty acid eutectic mixtures.

Fatty acid eutectics	Theoretically calculated eutectic mass ratios	Experimentally determined eutectic mass ratios
PA-SA	62.99/37.01	62.99/37.01
MA-PA-SA	56.82/28.08/15.1	56.82/28.08/15.1
LA-MA-PA-SA	55.24/25.43/12.57/6.76	63.24/20.89/10.32/5.55
CA-LA-MA-PA-SA	55.60/27.69/9.49/4.69/2.53	61.09/24.61/8.13/4.01/2.16

aluminum foil. The rotating speed of roller, voltage applied and working distance between needle tip and roller were fixed at 100 rpm, 12 kV and 12 cm, respectively.

2.4. Magnetron sputtering

Ag nanostructure films were deposited on the surface of electrospun PU fibers membranes by using JZCK-420B magnetron sputter coating system. High-purity Ag target (99.999%) were deployed for metallic coating of Ag at 0.5 Pa pressure with a power of 90 W. Argon (99.999%) was selected as the bombardment gas. The sputtering was achieved on either sides of the specimen at room temperature for 2 h, 6 h and 10 h each side, respectively. These coated PU samples were renamed as PU/Ag2, PU/Ag6 and PU/Ag10, respectively. During magnetron sputtering, the substrate holder was rotating at a speed of 100 rpm to ensure that sputtered particles were uniformly deposited on the surface of electrospun PU fibrous mats.

2.5. Physical adsorption

Electrospun PU fibers membranes with the size of 5 cm × 5 cm were immersed into molten quinary fatty acid eutectic for 24 h until saturated absorption, both before and after magnetron sputter of Ag. Saturated absorption showed that there was no significant change in the weight of the fibers membranes even after giving it more time in solution. Then the prepared phase change composite fibrous membranes samples treated with quinary fatty acid eutectic were hanged for 10 h at room temperature. The samples were recorded as CA-LA-MA-PA-SA/PU, CA-LA-MA-PA-SA/PU/Ag2, CA-LA-MA-PA-SA/PU/Ag6 and CA-LA-MA-PA-SA/PU/Ag10 composite PCMs, respectively.

2.6. Characterizations

The surface chemical compositions of prepared samples were analyzed by energy dispersive X-ray spectroscopy (EDX). The Nicolet iS10 FT-IR spectrometer was employed to determine the FTIR spectra of samples, which were recorded in the range of 400–4000 cm^{-1}. The surface morphologies of uncoated and Ag-coated electrospun PU fibers were examined by atomic force microscopy (AFM, Benyuan CSPM 5000). Scanning was carried out in tapping mode AFM. Scanning electron microscopy (Hitachi SU1510, SEM) was used to observe the morphological structures of the composite PCMs. Thermal energy storage properties of the fatty acid eutectic and composite PCMs were measured through differential scanning calorimetry instrument (DSC-Q200) with the scanning rate of 8 °C/min in nitrogen atmosphere. Additionally, 100 DSC thermal cycling tests of CA-LA-MA-PA-SA/PU/Ag10 composite PCMs were also performed with the scanning rate of 8 °C/min.

2.7. Thermal performance test

Thermal energy storage and retrieval rates of the synthesized composite PCMs were measured through the same experimental procedures as explained in our previous publications [17,18]. Firstly we cut samples into small pieces and then put into the glass bottle. Following to this, the thermocouple was inserted into the bottle that was tightly surrounded with the sample. The heating process was performed in a water bath at a constant temperature of 40 °C. When detected temperature was found stable at 35 °C by thermocouple, the glass bottle was instantly transferred to the refrigerator at −10 °C to subject the cooling process. The measured weight of each sample was around 10 g. During the measurements, temperature variations of two samples were automatically detected by PC via data logger with a temperature measuring accuracy of ±2 °C with 1 min of time interval. These measurements were repeated for 3 times and the average value was reported.

3. Results and discussion

3.1. EDX analysis

The deposited Ag on the surface of electrospun PU fibers membranes by sputter coating and adsorption of quinary fatty acid eutectics into porous network structure of Au-coated PU fibers membranes were determined by EDX analysis, as illustrated in Fig. 1. Similar characterization methods were also been reported in our previous research articles on electrospun Zn coated PA6 nanofibers [30] and TiO_2 coated PP nanofibers [31]. According to Fig. 1(a), the PU fibers without sputter coating were mainly composed of C and O element. And the peak intensity of O elements was notably weaker than that of C elements in the spectrum. In comparison to the original PU fibers, Ag-coated PU fibers with different coating times had considerably high Ag contents, as shown in Fig. 1 (b), (c) and (d), which can be attributed to the covering of the Ag nanoclusters on the PU fibers surface after sputter coating. The peak intensity of Ag elements was significantly stronger as compared to C elements. In other words, there can only be found very few weak peaks corresponding to C element in Fig. 1 (b) and (c). In this case, it was quite difficult to observe the relatively weaker symbol peak of O element. And with the increase of coating time (see Fig. 1(d)), the C and O elements belonged to the PU molecular have disappeared because the Ag nanoparticles were uniformly covered on the surface of electrospun PU fibers. The C and O elements cannot be detected due to the compact Ag nanolayer covered on the fiber surface. These results were similar to the observations of SEM and AFM images. Additionally, Ag elements have disappeared after physical adsorption and a large amount of C and O element on the surface of Ag-coated PU fibers can be seen from Fig. 1(e), which indicated that the quinary fatty acid eutectics were successfully combined into the three-dimensional network structure of Ag-coated PU fibers membranes during physical adsorption process.

3.2. FT-IR analysis characterization

In order to determine the chemical compatibility and interaction between CA-LA-MA-PA-SA quinary fatty acid eutectics and electrospun PU fibers membranes both before and after sputter

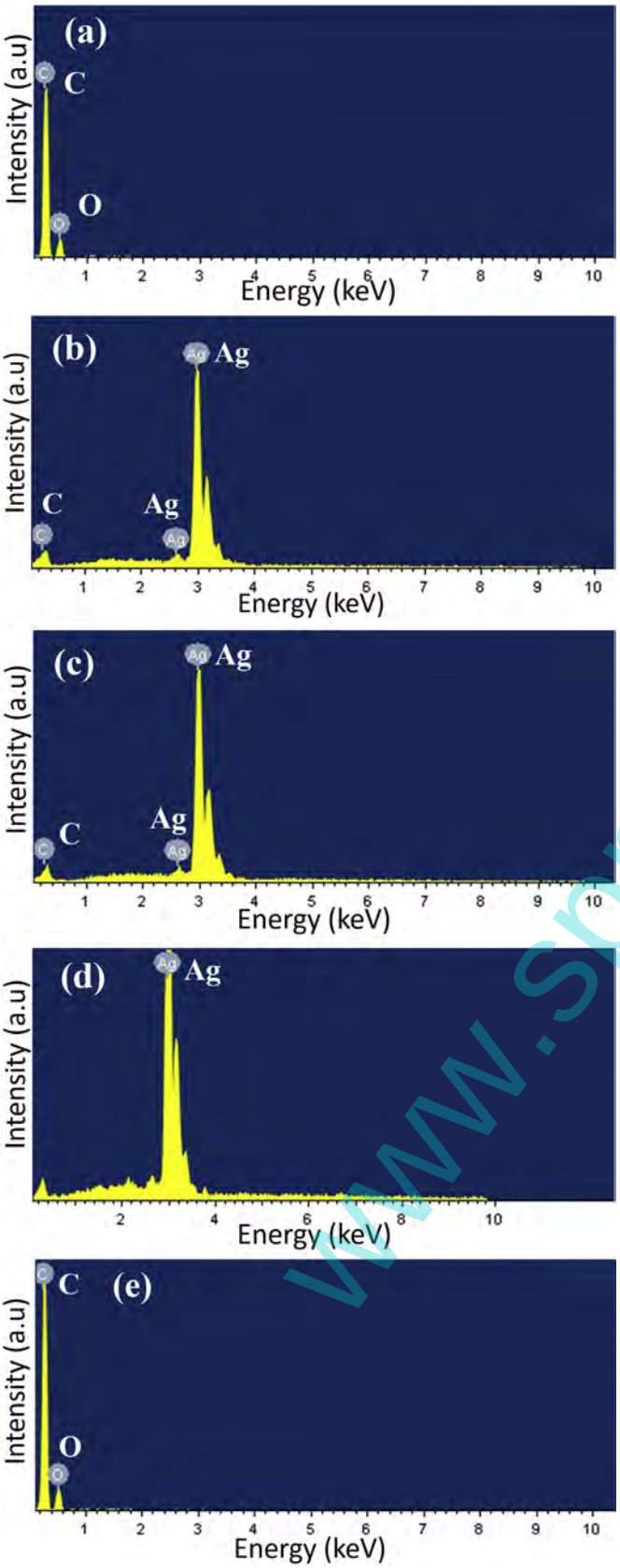

Fig. 1. EDX spectra of (a) PU, (b) PU/Ag2, (c) PU/Ag6 and (d) PU/Ag10 fibers membranes, as well as (e) the CA-LA-MA-PA-SA/PU/Ag10 composite PCMs.

coating of Ag, the FT-IR analysis was carried out. The FT-IR spectra of CA-LA-MA-PA-SA quinary fatty acid eutectics, un-coated and Ag-coated PU fibers, as well as the synthesized composite PCMs are shown in Fig. 2. It can be seen from Fig. 2(a) that the spectrum of electrospun PU fibers had strong absorption peaks at 3336 cm^{-1}, 2953 cm^{-1}, 2868 cm^{-1} corresponding to the stretching vibrations of *N*—H groups, asymmetric and symmetric stretching vibrations of *C*—H bond, respectively. Besides these bands, there were also five characteristic absorption peaks attributing to the stretching vibrations of C═O and *C*—O groups, *C*—C stretch vibration, *C*—H aromatic in-plane deformation as well as *C*—H aromatic out of pane deformation at the wave numbers of 1727 cm^{-1}, 1164 cm^{-1}, 1529 cm^{-1}, 1219 cm^{-1} and 769 cm^{-1}, respectively [32–34]. For the spectrum of CA-LA-MA-PA-SA quinary fatty acid eutectics (see Fig. 2(b)), the important characteristic peaks at 1707 cm^{-1}, 1281 cm^{-1} and 932 cm^{-1} were assigned to stretching vibrations of C═O, *C*—O and —OH bonds of carboxyl groups (-COOH), respectively. Moreover, there were four obvious absorption bands at about 2922 cm^{-1}, 2853 cm^{-1}, 1465 cm^{-1} and 721 cm^{-1}, which were regarded to the asymmetric and symmetric stretching vibrations of *C*—H bond, as well as the CH_2 or CH_3 deformation vibration and the rocking vibration in $(-CH_2-)_n$ ($n \geq 4$) groups, respectively. As compared to Fig. 2(a) and (b), in Fig. 2(c) we could not found any new significant characteristic absorption peaks, which indicated that the CA-LA-MA-PA-SA quinary eutectics and PU fibers membranes had no chemical reaction between them. In addition to this, in the spectrum of CA-LA-MA-PA-SA/PU composite fibers membranes, the absorption peaks of CA-LA-MA-PA-SA quinary fatty acid eutectics are in the interval of 1600—650 cm^{-1} that could perfectly overlap with the absorption bands of PU fibers, which also proposes that CA-LA-MA-PA-SA quinary eutectics and electrospun PU matrices had good compatibility in those composite fibers. However, as shown in Fig. 2(d), that all absorption peaks of PU molecular disappeared in the spectrum of Ag-coated PAN fibers, demonstrating that the Ag nanolayers have been successfully coated on the surface of PU fibers after sputter coating. Furthermore, the peak positions of the CA-LA-MA-PA-SA/PU/Ag composite fibers coincided with those of CA-LA-MA-PA-SA quinary fatty acid eutectics, illustrating that the CA-LA-MA-PA-SA quinary fatty acid eutectics have been physically adsorbed into three-dimensional porous network structure of Ag-coated PU fibers membranes.

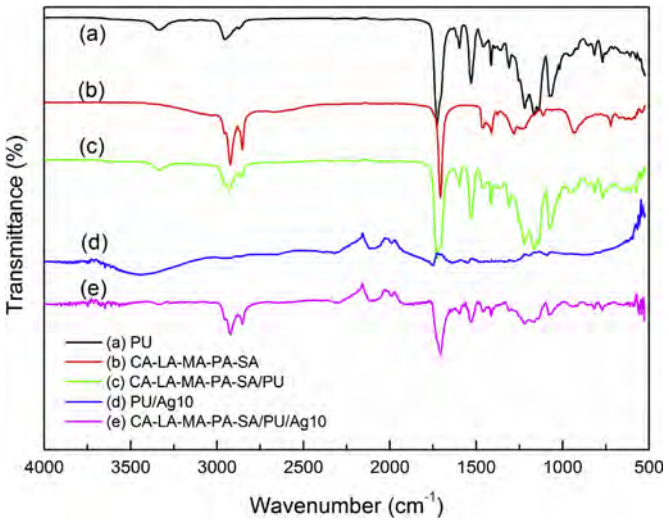

Fig. 2. FT-IR spectra of (a) electrospun PU fibers membrane, (b) CA-LA-MA-PA-SA eutectic, (c) CA-LA-MA-PA-SA/PU composite PCMs, (d) PU/Ag10 fibers membrane and (e) CA-LA-MA-PA-SA/PU/Ag10 composite PCMs.

3.3. Morphology and structure

In order to investigate the effect of Ag nanolayers on morphological structure of the synthesized PU supporting materials and composite PCMs, the morphological structures of electrospun PU fibrous membranes and CA-LA-MA-PA-SA/PU composite phase change fibrous membranes both before and after sputter coating of Ag were examined by AFM and SEM analysis.

3.3.1. AFM scanning

As presented in Fig. 3, the AFM images obtained at higher magnification clearly showing significant differences in surface morphological features between uncoated and Ag-coated PU fibers. It can be observed in Fig. 3(a) that the surface of electrospun PU fibers appeared to be relatively smooth without any particles on their surface, while the Ag-coated PU fibers with different coating time exhibited relatively coarse and rough surfaces with shallow grooves (see Fig. 3(b) and (c)). Moreover, it is noteworthy that the surface roughness of PU fibers gradually increased with the expansion of sputter coating time due to the gradual growth of the Ag nanoclusters on the surface of PU fibers during magnetron sputtering process. According to AFM images, it was also concluded that the metallic Ag nanoparticles had been successfully aggregated and deposited on the surface of PU fibers.

3.3.2. SEM observation

Scanning electron microscopy images of uncoated and Ag-coated PU fibers membranes are shown in Fig. 4 and Fig. 5. Fig. 4, illustrated a significant increase in the average fiber diameter of Ag-coated PU fibers from 1 μm to 4.8 μm. The surface roughness of PU fibers dramatically increased with the increase in coating time. The SEM images showed that the large amounts of Ag nanoparticles had been covered on the surface of PU fibers after sputter coating. Thereafter, the Ag-coated PU membranes with different coating times were selected as supporting materials to absorbed quinary fatty acid eutectic through the action of capillary absorption, surface tension forces and nanoconfinement effects. Morphological structure of the prepared composite PCMs were also inspected under SEM, and the images were shown in Fig. 5. It can be found from Fig. 5 that there was a clear difference between the morphological structure of fibers membranes before and after physical adsorption, demonstrating that the CA-LA-MA-PA-SA eutectic had been successfully absorbed and promoted by the three-dimensional porous network structure of uncoated and Ag-coated PU supporting matrices. It was notable that the composite PCMs could well-retain their overall shapes after adsorption, even though the SEM operating temperature was higher than the phase change temperature of CA-LA-MA-PA-SA quinary eutectic. In other words, the supporting materials could efficiently prevent the fluidity at the temperature beyond the melting point of eutectic to overcome liquid leakage problem. Moreover, the Ag-coated PU membranes could also provide the mechanical strength to the phase change systems. Therefore, it is envisioned that this type of form-stable composite PCMs could be particularly useful for the application related to the storage and retrieval of thermal energy.

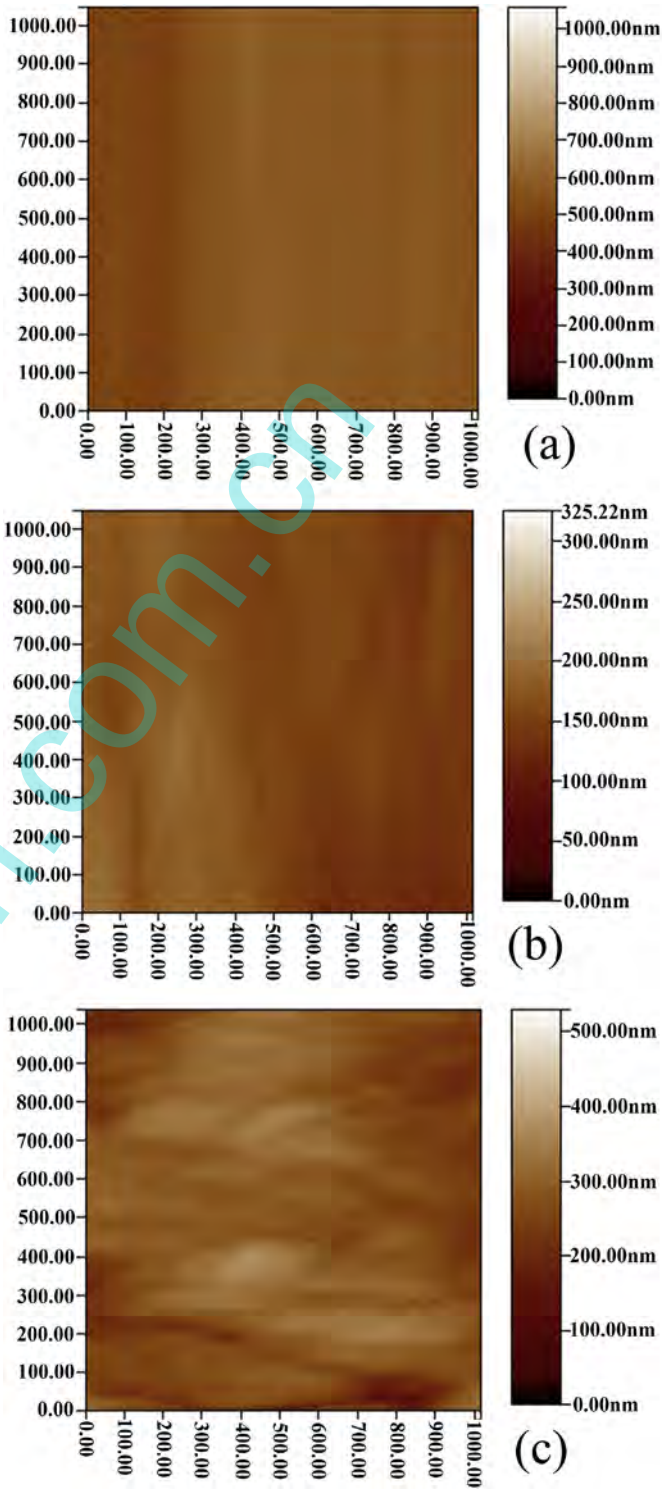

Fig. 3. AFM images of (a) PU, (b) PU/Ag2 and (c) PU/Ag10 fibers membranes.

3.4. DSC analysis

Multiple fatty acid eutectic is a mixture of two or more components of fatty acid, which can be selected as a new kind of solid-liquid PCMs because each fatty acid in the mixture solution, could melt or freeze synchronously during phase change processes. Fig. 6 shows the DSC curves of synthesized binary, ternary, quaternary and quinary fatty acid eutectics during heating and cooling processes. Moreover, the phase change curves of un-coated and Ag-coated PU membranes, and composite PCMs during DSC testing processes are also presented in Fig. 7. The corresponding data of their thermal properties are summarized in Table 3. As shown in Fig. 6, there was only one single endothermic and exothermic peak for the four types of fatty acid eutectics, indicating that the binary, ternary, quaternary and quinary fatty acid eutectics were successfully synthesized according to the lowest eutectic point theory. Additionally, it can be found that the phase change temperatures

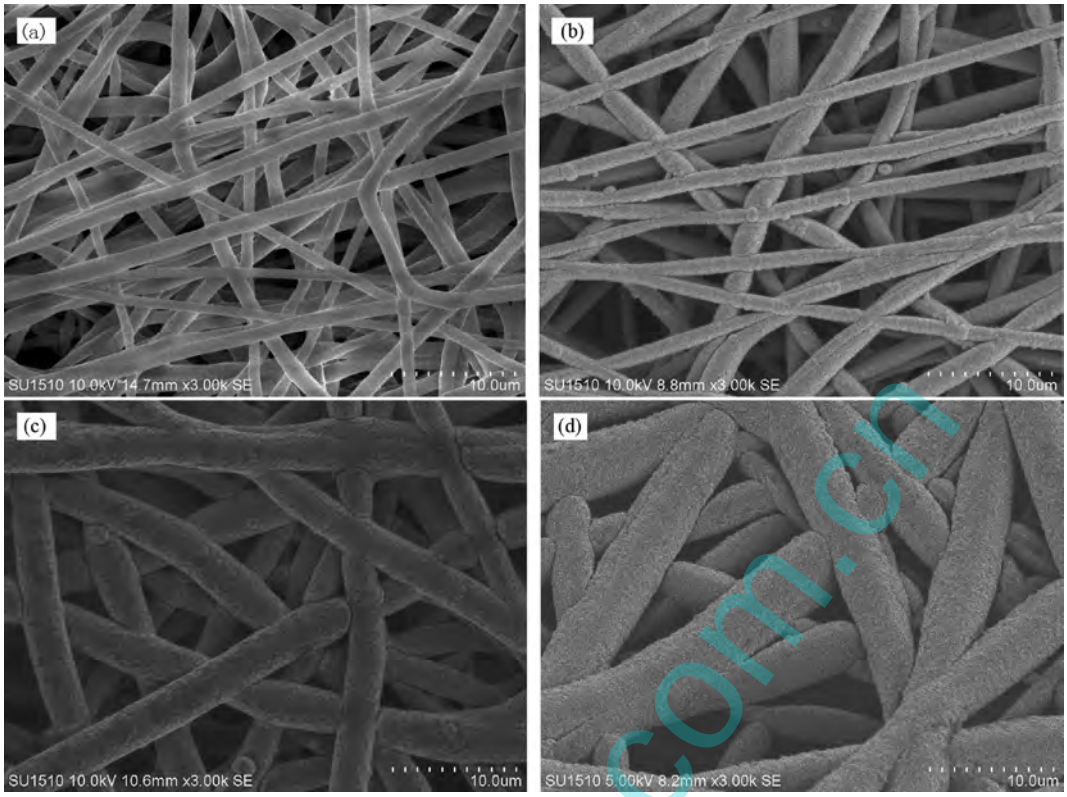

Fig. 4. SEM images of fibers membranes: (a) PU, (b) PU/Ag2, (c) PU/Ag6 and (d) PU/Ag10.

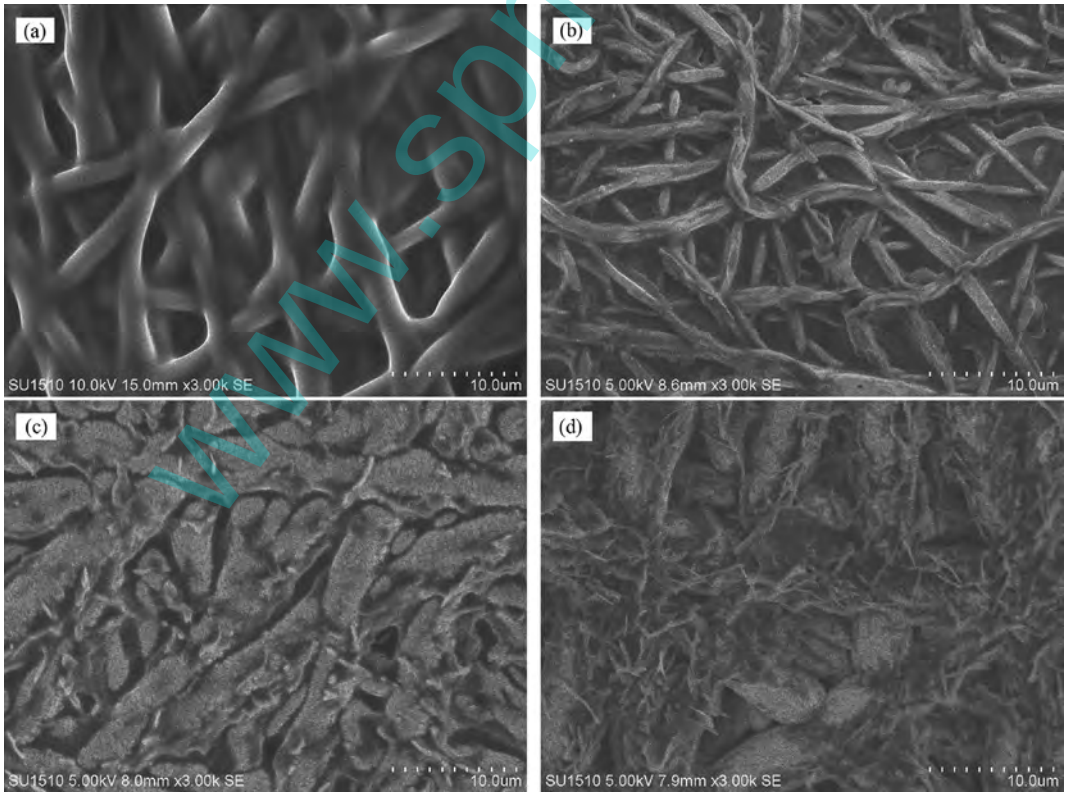

Fig. 5. SEM images of composite PCMs: (a) CA-LA-MA-PA-SA/PU, (b) CA-LA-MA-PA-SA/PU/Ag2, (c) CA-LA-MA-PA-SA/PU/Ag6 and (d) CA-LA-MA-PA-SA/PU/Ag10.

and enthalpies of the synthesized fatty acid eutectics gradually decreased with the increase in the components of fatty acid in eutectic mixtures. It is worthwhile to note that pristine fatty acids performed supercooling to some extent, but this supercooling

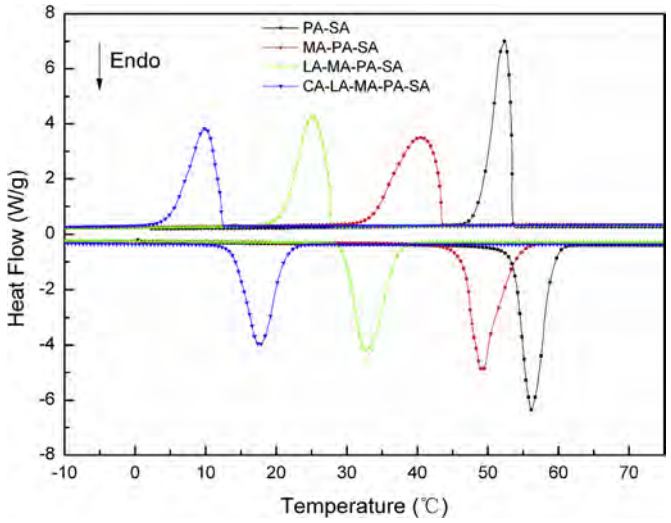

Fig. 6. DSC curves of the prepared binary, ternary, quaternary, quinary fatty acid eutectics.

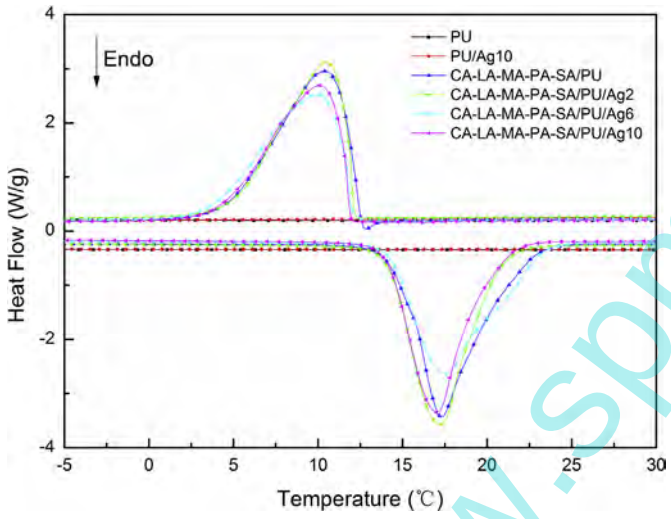

Fig. 7. DSC curves of electrospun PU fibers membrane, PU/Ag10 membranes and composite PCMs.

Table 3
The peak onset temperature (T_e), melting peak temperature (T_m), freezing peak temperature (T_c), melting enthalpy (ΔH_m) and freezing enthalpy (ΔH_c) of the prepared binary, ternary, quaternary, quinary fatty acid eutectics and composite PCMs.

Fatty acid eutectics	Melting			Freezing		
	T_e (°C)	T_m (°C)	ΔH_m (kJ/kg)	T_e (°C)	T_c (°C)	ΔH_c (kJ/kg)
PA-SA	53.69	56.16	204.7	53.45	52.43	204.2
MA-PA-SA	46.69	49.23	170.3	43.45	40.42	168.7
LA-MA-PA-SA	29.64	32.72	151.9	27.66	25.13	149.0
CA-LA-MA-PA-SA	14.04	17.64	132.8	12.36	9.95	129.8
CA-LA-MA-PA-SA/PU	14.91	17.31	110.6	12.57	10.40	110.6
CA-LA-MA-PA-SA/PU/Ag2	14.12	17.22	106.3	12.13	10.47	106.0
CA-LA-MA-PA-SA/PU/Ag6	14.18	17.58	101.1	11.98	9.95	100.4
CA-LA-MA-PA-SA/PU/Ag10	14.08	16.99	97.93	11.87	10.07	97.24

performance have not been observed from the DSC curves of the synthesized binary, ternary, quaternary and quinary fatty acid eutectics. Therefore, the prepared multielement fatty acid eutectics were more suitable for thermal energy storage applications. The DSC results suggested that the CA-LA-MA-PA-SA quinary eutectic can be considered as an innovation solid-liquid PCM for lower temperature thermal storage applications. Here it can be concluded that phase change temperatures of fatty acids could be effectively adjusted to the values of actual climatic requirements by preparing the multielement fatty acid eutectics. Moreover, the successful preparation of multiple fatty acid eutectics also certainly expanded the applications of fatty acids as PCMs.

It was observed from Fig. 7 that there was no phase transition peak for uncoated and Ag-coated PU membranes, which indicated that the supporting membranes had no contribution to heat storage capability of phase change systems. According to Table 3, there was no significant changes in the phase change temperatures of the composite PCMs with increasing coating time. Although the intensity of endothermic and exothermic peaks of composite PCMs slightly declined with the increase of Ag content, these composite PCMs still possessed excellent thermal energy storage capability because their phase change enthalpies were ranging from about 110 kJ/kg to 97 kJ/kg (see Table 3). Moreover, the melting enthalpies of composite PCMs were very close to their freezing enthalpies, which also demonstrated that these composite PCMs were a kind of transition reversible latent storage materials.

The adsorption ratios can be calculated by melting or freezing enthalpy of composite PCMs divided by the melting or freezing enthalpy of quinary fatty acid eutectic. According to melting enthalpies, the calculated adsorption ratios were respectively determined at 83.18%, 80.04%, 76.13% and 73.74% for CA-LA-MA-PA-SA/PU, CA-LA-MA-PA-SA/PU/Ag2, CA-LA-MA-PA-SA/PU/Ag6 and CA-LA-MA-PA-SA/PU/Ag10, which might be due to the increased average fiber diameters, decreased pore diameters, declined specific surface area and incremental Ag quantities of Ag-coated PU membranes comparing with original PU membranes. On the basis of the above findings from DSC analysis, it can be concluded that the phase change enthalpies of synthesized composite PCMs were slightly reduced with the increase of Ag coating time, whereas there was no appreciable impact on the phase transition temperatures.

Fig. 8 shows the 100 cycles of DSC thermal curves of CA-LA-MA-PA-SA/PU/Ag10 composite PCMs. It can be found from Fig. 8 that the phase change temperatures and enthalpies of CA-LA-MA-PA-SA/PU/Ag composite PCMs can be remained very well after 100 times melting and freezing processes, which exhibited that by combining the Ag with nanofibrous mats had no massive effect on thermal cycling reliability of form-stable composite PCMs. On the basis of the above conducted DSC analysis, it can be concluded that the synthesized form-stable composite PCMs in this study displayed high phase change enthalpies, lower phase change temperatures and thermal reliability and these composite PCMs can be a potential candidate for thermal energy storage, building energy storage materials and thermal regulating textiles applications.

3.5. Heat storage and release properties

The heat storage and release property of form-stable PCMs is a key factor that affects their applications. Low thermal storage and release rates of PCMs could lead to the poor thermal energy utilization efficiency. Therefore, form-stable PCMs with high heat transfer rates are appreciated for the application related to the thermal energy storage and release. In this paper, magnetron sputter coating was considered as a novel method to produce Ag nanolayers with high thermal conductivity in phase change system to improve the thermal storage and release rates of form-stable PCMs. The typical temperature-time curves of CA-LA-MA-PA-SA/PU/Ag form-stable composite PCMs with different sputter coating

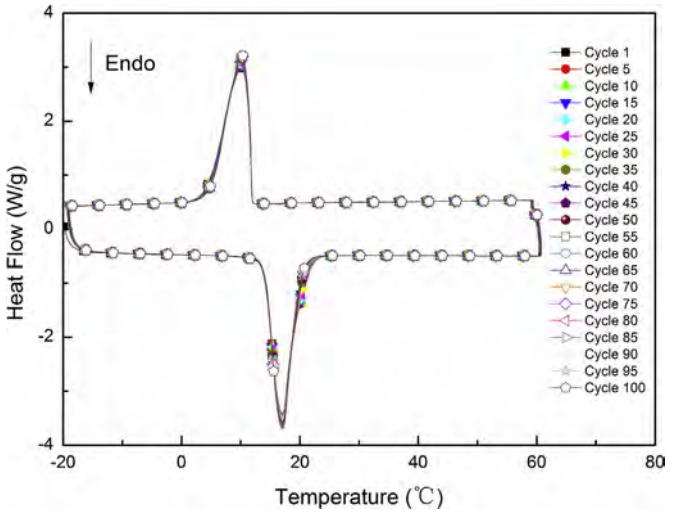

Fig. 8. DSC cycle curves of the CA-LA-MA-PA-SA/PU/Ag10 form-stable composite PCMs.

time during melting and freezing processes are displayed in Fig. 9. The interval time between the same initial temperature (about −5 °C) and the melting peak temperature (about 17 °C) was determined as the melting time from the heating curve. The freezing time was defined from the cooling curve, as the interval time from initial temperature (about 35 °C) to the freezing peak temperature of the samples at approximately 10 °C. The measurement results indicated that the CA-LA-MA-PA-SA/PU/Ag composite PCMs showed higher melting and freezing rates than those of CA-LA-MA-PA-SA/PU composite PCMs, and the thermal transfer rates of CA-LA-MA-PA-SA/PU/Ag composite PCMs were also became higher with the increase in coating times, which revealed that the heat transfer rates were significantly boosted by depositing Ag nanostructure films on the surface of PU fibers membranes. During the melting process, it took about 9.5 min for CA-LA-MA-PA-SA/PU composite PCMs to raise its temperature from −5 °C to 35 °C, whereas only about 7.5 min, 4.3 min and 3.3 min were required for the CA-LA-MA-PA-SA/PU/Ag2, CA-LA-MA-PA-SA/PU/Ag6 and CA-LA-MA-PA-SA/PU/Ag10 composite PCMs. Moreover, the freezing time were reduced from 35.1 min (CA-LA-MA-PA-SA/PU) to 27.1 min (CA-LA-MA-PA-SA/PU/Ag2), 25.6 min (CA-LA-MA-PA-SA/PU/Ag6) and 21.9 min (CA-LA-MA-PA-SA/PU/Ag10) respectively with temperature dropping down from 35 °C to −5 °C. It was clear that the melting (freezing) times declined by 21% (23%), 55% (27%) and 65% (38%) for CA-LA-MA-PA-SA/PU/Ag2, CA-LA-MA-PA-SA/PU/Ag6 and CA-LA-MA-PA-SA/PU/Ag10 composite PCMs, respectively. From above mentioned outcomes, it can be interpreted that the formation of continuous thermal conducting networking or/and heat conductive bridges would help to provide an efficient percolating path for heat flow in composite PCMs due to the covered Ag films on the surface of PU fibers membranes. In other words, the Ag nanostructure films with the higher thermal conductivity in the phase change systems accelerated the heat transfer rates of CA-LA-MA-PA-SA eutectic during phase change processes. Therefore, with different coating times the change in temperature of CA-LA-MA-PA-SA/PU/Ag composite PCMs were sharper than those of CA-LA-MA-PA-SA/PU composite PCMs. The results also revealed that the incorporation of Ag nanostructure films into the phase change systems was an effective method to improve the thermal storage and release properties of form-stable PCMs.

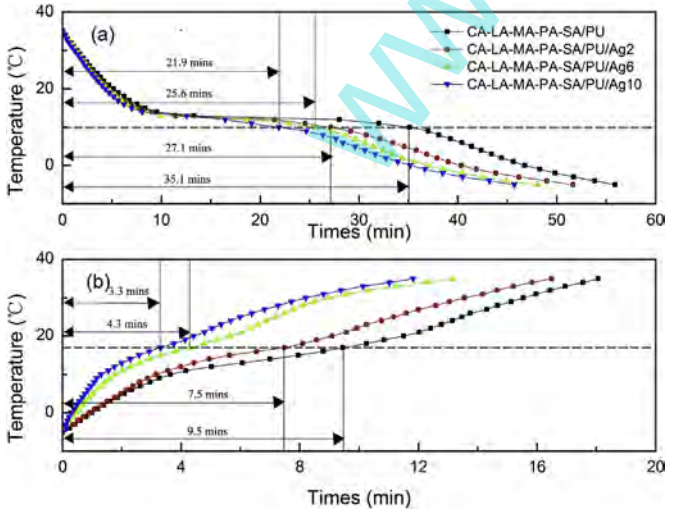

Fig. 9. Temperature-time curves acquired from thermal performance tests of form-stable composite PCMs: (a) heat release and (b) heat storage.

4. Conclusions

A series of innovative CA-LA-MA-PA-SA/PU/Ag composite PCMs were successfully synthesized through electrospinning and magnetron sputtering followed by physical adsorption, in which the CA-LA-MA-PA-SA quinary fatty acid eutectics acted as solid-liquid PCMs and Ag-coated PU fibers membranes selected as the supporting material. The EDX results confirmed that the Ag nanoparticles have been successfully deposited on the surface of electrospun PU fibers membranes. The AFM examination illustrated that the surface roughness of the PU fibers significantly became higher with the increase in coating time. The SEM images showed that the CA-LA-MA-PA-SA eutectics were well adsorbed and dispersed in three-dimensional porous network structures of uncoated and Ag-coated PU fibers membranes due to the capillary action and surface tension forces. The DSC analysis suggested that there was a rapid decline in the phase change temperatures of fatty acid eutectics with the rise of components (i.e., fatty acid types) in the eutectics. Although the phase change enthalpies and adsorption ratios of composite PCMs slightly decreased with the increase in Ag coating time, the composite PCMs still exhibited high phase change enthalpies from 110.6 kJ/kg to 97.93 kJ/kg. All composite PCMs exhibited suitable phase change temperatures for actual climatic requirements within the range of 3.82 °C—21.15 °C. The results from thermal performance test indicated that the heat storage and release rates of the CA-LA-MA-PA-SA/PU/Ag composite PCMs also increased with augment amount of Ag, which demonstrating that magnetron sputtering was a useful method to enhance the thermal energy transfer efficiency of phase change systems. Based on all results, it was concluded that the synthesized CA-LA-MA-PA-SA/PU/Ag composites PCMs having proper phase change temperatures, excellent thermal reliability, high latent heat and thermal transfer efficiency can be regarded as innovative form-stable PCMs for lower temperature thermal energy storage applications such as energy-efficient building materials and thermo-regulating textiles.

Acknowledgements

This research was financially supported by the National High-tech R&D Program of China (No.2012AA030313), Changjiang Scholars and Innovative Research Team in University (No.IRT1135), the Priority Academic Program Development of Jiangsu Higher Education Institutions, Industry-Academia-Research Joint

Innovation Fund of Jiangsu Province (BY2012068), Science and Technology Support Program of Fujian Province (JK2014042).

References

[1] A.G. Entrop, H.J.H. Brouwers, A.H.M.E. Reinders, Experimental research on the use of micro-encapsulated phase change materials to store solar energy in concrete floors and to save energy in dutch houses, Sol. Energy 85 (2011) 1007–1020.

[2] Y.B. Seong, J.H. Lim, Energy saving potentials of phase change materials applied to light weight building envelopes, Energies 6 (2013) 5219–5230.

[3] J. Jeon, S.G. Jeong, J.H. Lee, J. Seo, S. Kim, High thermal performance composite PCMs loading xGnP for application to building using radiant floor heating system, Sol. Energ Mater. Sol. Cells 101 (2012) 51–56.

[4] A.F. Regin, S.C. Solanki, J.S. Saini, Heat transfer characteristics of thermal energy storage system using PCM capsules: a review, Renew. Sust. Energy Rev. 12 (2008) 2438–2458.

[5] W. Lu, S.A. Tassou, Characterization and experimental investigation of phase change materials for chilled food refrigerated cabinet applications, Appl. Energy 112 (2013) 1376–1382.

[6] K. Lafdi, O. Mesalhy, A. Elgafy, Graphite foams infiltrated with phase change materials as alternative materials for space and terrestrial thermal energy storage applications, Carbon 46 (2008) 159–168.

[7] M. Mazman, L.F. Cabeza, H. Mehling, M. Nogues, H. Evliya, H.O. Paksoy, Utilization of phase change materials in solar domestic hot water systems, Renew. Energy 34 (2009) 1639–1643.

[8] A. Najjar, A. Hasan, Modeling of greenhouse with PCM energy storage, Energy Convers. Manage. 49 (2008) 3338–3342.

[9] P. Goli, S. Legedza, A. Dhar, R. Salgado, J. Renteria, A.A. Balandin, Graphene-enhanced hybrid phase change materials for thermal management of Li-ion batteries, J. Power Sources 248 (2014) 37–43.

[10] A. Sharma, V.V. Tyagi, C.R. Chen, D. Buddhi, Review on thermal energy storage with phase change materials and applications, Renew. Sust. Energy Rev. 13 (2009) 318–345.

[11] Y.P. Yuan, N. Zhang, W.Q. Tao, X.L. Cao, Y.L. He, Fatty acids as phase change materials: a review, Renew. Sust. Energ Rev. 29 (2014) 482–498.

[12] L.J. Wang, D. Meng, Fatty acid eutectic/polymethyl methacrylate composite as form-stable phase change material for thermal energy storage, Appl. Energy 87 (2010) 2660–2665.

[13] A. Sari, C. Alkan, A. Altintas, Preparation, characterization and latent heat thermal energy storage properties of micro-nonencapsulated fatty acids by polystyrene shell, Appl. Therm. Eng. 73 (2014) 1160–1168.

[14] M. Silakhori, H.S.C. Metselaar, T.M.I. Mahlia, H. Fauzi, S. Baradaran, M.S. Naghavi, Palmitic acid/polypyrrole composites as form-stable phase change materials for thermal energy storage, Energy Convers. Manage. 80 (2014) 491–497.

[15] K. Tumirah, M.Z. Hussein, Z. Zulkarnain, R. Rafeadah, Nano-encapsulated organic phase change material based on copolymer nanocomposites for thermal energy storage, Energy 66 (2014) 881–890.

[16] Y. Konuklu, H.O. Paksoy, M. Unal, S. Konuklu, Microencapsulation of a fatty acid with Poly (melamine–urea–formaldehyde), Energy Convers. Manage. 80 (2014) 382–390.

[17] Y.B. Cai, C.T. Gao, T. Zhang, Z. Zhang, Q.F. Wei, J.M. Du, Y. Hu, Song Lei. Influences of expanded graphite on structural morphology and thermal performance of composite phase change materials consisting of fatty acid eutectics and electrospun PA6 nanofibrous mats, Renew. Energy 57 (2013) 163–170.

[18] H.Z. Ke, Z.Y. Pang, Y.F. Xu, X.D. Chen, J.P. Fu, Y.B. Cai, F.L. Huang, Q.F. Wei, Graphene oxide improved thermal and mechanical properties of electrospun methyl stearate/polyacrylonitrile form-stable phase change composite nanofibers, J. Therm. Anal. Calorim. 117 (2014) 109–122.

[19] A. Karaipekli, A. Sari, K. Kaygusuz, Thermal conductivity improvement of stearic acid using expanded graphite and carbon fiber for energy storage applications, Renew. Energy 32 (2007) 2201–2210.

[20] T. Wei, B. Zheng, J. Liu, Y.F. Gao, W.H. Guo, Structures and thermal properties of fatty acid/expanded perlite composites as form-stable phase change materials, Energ Build. 68 (2014) 587–592.

[21] S.Y. Liu, H.M. Yang, Stearic acid hybridizing coal–series kaolin composite phase change material for thermal energy storage, Appl. Clay Sci. 101 (2014) 277–281.

[22] S.K. Song, L.J. Dong, S. Chen, H.A. Xie, C.X. Xiong, Stearic–capric acid eutectic/activated-attapulgiate composite as form-stable phase change material for thermal energy storage, Energy Convers. Manage. 81 (2014) 306–311.

[23] Y. Wang, H. Zheng, H.X. Feng, D.Y. Zhang, Effect of preparation methods on the structure and thermal properties of stearic acid/activated montmorillonite phase change materials, Energ Build. 47 (2012) 467–473.

[24] G.Y. Fang, H. Li, Z. Chen, X. Liu, Preparation and properties of palmitic acid/SiO_2 composites with flame retardant as thermal energy storage materials, Sol. Energ Mater. Sol. Cells 95 (2011) 1875–1881.

[25] M. Mehrali, S.T. Latibari, M. Mehrali, T.M.I. Mahlia, E. Sadeghinezhad, H.S.C. Metselaar, Preparation of nitrogen-doped graphene/palmitic acid shape stabilized composite phase change material with remarkable thermal properties for thermal energy storage, Appl. Energy 135 (2014) 339–349.

[26] Q.F. Wei, Q.X. Xu, Y.B. Cai, Y.Y. Wang, Evaluation of interfacial bonding between fibrous substrate and sputter coated copper, Surf. Coat. Tech. 202 (2008) 4673–4680.

[27] Q.F. Wei, X.L. Xiao, D.Y. Hou, H. Ye, F.L. Huang, Characterization of nonwoven material functionalized by sputter coating of copper, Surf. Coat. Tech. 202 (2008) 2535–2539.

[28] Y.P. Yuan, W.Q. Tao, X.L. Cao, L. Bai, Theoretic prediction of melting temperature and latent heat for a fatty acid eutectic mixture, J. Chem. Eng. Data 56 (2011) 2889–2891.

[29] A. Sari, H. Sari, A. Onal, Thermal properties and thermal reliability of eutectic mixtures of some fatty acids as latent heat storage materials, Energy Convers. Manage. 45 (2004) 365–376.

[30] Q.F. Wei, Q.X. Xu, Y.B. Cai, W.D. Gao, C.Z. Bo, Characterization of polymer nanofibers coated by reactive sputtering of zinc, J. Mater. Process Tech. 209 (2009) 2028–2032.

[31] Q.F. Wei, L.Y. Yu, R.R. Mather, X.Q. Wang, Preparation and characterization of titanium dioxide nanocomposite fibers, J. Mater. Sci. 42 (2007) 8001–8005.

[32] A.R. Unnithan, N.A.M. Barakat, P.B. Tirupathi Pichiah, G. Gnanasekaran, R. Nirmala, Y.S. Cha, C.H. Jung, M. El-Newehy, H.Y. Kim, Wound-dressing materials with antibacterial activity from electrospun polyurethane-dextran nanofiber mats containing ciprofloxacin HCl, Carbohydr. Polym. 90 (2012) 1786–1793.

[33] B.R. Nair, C.G. Gregoriou, P.T. Hammond, FT-IR studies of side chain liquid crystalline thermoplastic elastomers, Polymer 41 (2000) 2961–2970.

[34] H.Z. Liu, S.X. Zheng, Polyurethane networks nanoreinforced by polyhedral oligomeric silsesquioxane, Macromol. Rapid Comm. 26 (2005) 196–200.